JACS
JOURNAL OF THE AMERICAN CHEMICAL SOCIETY
Communication
pubs.acs.org/JACS

Probing the Surface of Colloidal Nanomaterials with Potentiometry *in Situ*

Igor Fedin[†] and Dmitri V. Talapin*[,†,‡]

[†]Department of Chemistry and James Franck Institute, The University of Chicago, Chicago, Illinois 60637, United States
[‡]Center for Nanoscale Materials, Argonne National Laboratory, Argonne, Illinois 60439, United States

Supporting Information

ABSTRACT: Colloidal nanomaterials represent an important branch of modern chemistry. However, we have very little understanding of molecular processes that occur at the nanocrystal (NC) surface during synthesis and post-synthetic modifications. Here we show that potentiometry can be used to study the surface of colloidal NCs under realistic reaction conditions. Potentiometric titrations of CdSe and InP nanostructures provide information on the active surface area, the affinity of ligands to the NC surface, and the surface reaction kinetics. These studies can be carried out at different temperatures in polar and nonpolar media for NCs of different sizes and shapes. *In situ* potentiometry can provide real-time feedback during synthesis of core−shell nanostructures.

Colloidally synthesized nanocrystals (NCs) are used in light-emitting diodes,[1] transistors,[2] solar cells,[3] and other devices as well as in bioimaging tags,[4] catalysts,[5] etc. All these applications require optimizations of NC size, shape, composition, and surface chemistry.[6] Despite enormous progress in NC synthesis, we are still lacking ability to fully characterize NC surfaces, especially in solution. NCs containing 10^2−10^5 atoms are too large to be studied with atomic precision by single-crystal X-ray techniques. On the other hand, they are too small for traditional surface science techniques[7,8] used to study the surface of bulk crystals.

It would be particularly useful to monitor NC surfaces *in situ* during NC synthesis or surface modifications. General examples of *in situ* monitoring extend from the common chemistry (e.g., monitoring pH during chemical reaction) to the fabrication of semiconductor devices (e.g., using reflection high-energy electron diffraction, RHEED, to monitor deposition of atomic layers in molecular beam epitaxy).[8] In the field of colloidal NCs, however, *in situ* monitoring is still under development. Few reported examples include *in situ* fluorescence[9] and UV−vis absorption spectroscopy,[10] FTIR,[11] NMR,[12] synchrotron SAXS, and XANES.[13] These techniques often lack an easily interpretable relationship between analytical signal and surface chemistry (as in optical spectroscopy) or require sophisticated equipment (as in synchrotron-based SAXS and XANES).

We propose potentiometry as a surface-sensitive, non-destructive, fast, and inexpensive technique to probe NC surfaces *in situ*. Easy to set up and interpret, this approach can be used for online analyses during NC syntheses. An apparent complication comes from the fact that the majority of functional nanomaterials are synthesized and handled in nonpolar solvents that cannot dissolve the supporting electrolytes needed for recording electrode potentials. Here we address this problem for colloidal NCs with inorganic surface ligands[14,15] dispersed in a polar solvent; we also derive conditions for potentiometric studies of NCs with traditional organic surface ligands.

In the present work we use NCs of technologically important CdSe and InP semiconductors. CdSe quantum dots (QDs) were synthesized by modified literature methods[16,17] using trioctylphosphine oxide, trioctylphosphine, oleic acid, and oleylamine as capping ligands (Figure 1A). We then used Me_3OBF_4 to strip these organic ligands and obtain "bare" NCs colloidally stabilized by positive surface charge counterbalanced by BF_4^- ions in DMF.[15,17] These NCs, further referred to as $[CdSe/Cd^{2+}]^{n+}nBF_4^-$, were redispersed in *N*-methylformamide (NMF) and titrated with a 0.01 M solution of K_2S in NMF. The concentration of sulfide ions in equilibrium with the surface of colloidal NCs was monitored using a Ag wire coated with Ag_2S film as a Ag|Ag_2S ion-selective electrode[18] with a nonaqueous Ag|Ag(crypt) reference electrode.[19] Titration of a $Cd(NO_3)_2$ solution in NMF with K_2S in NMF showed the expected electrode response (Figure S3).

First, to test the reliability of this technique with respect to NC colloids, we titrated three aliquots—1.22, 2.44, and 3.66 mg—of 4.3 nm $[CdSe/Cd^{2+}]^{n+}nBF_4^-$ NCs with 0.01 M K_2S in NMF (Figure 1B). As titration progressed, a slow decrease of the electrode potential was followed by an abrupt jump in the vicinity of the inflection point. For the simplest adsorption model, the Langmuir isotherm, the inflection point of the titration curve coincides with the equivalence point (where the amount of added titrant matches the amount required to cover all adsorption sites). As expected, the equivalent amount of the titrant was proportional to the amount of the QDs taken for the titration (Figure 1B, inset). We can then calculate the total amount of CdSe materials from solution absorption at 350 nm, where the molar extinction coefficient of CdSe QDs is size-independent and simply proportional to the number of CdSe molecular units.[20] The equivalent number of moles of S^{2-} constitutes 18.4 ± 0.6% of total CdSe substance, which is somewhat lower than the total fraction of surface atoms for 4.3 nm CdSe QDs (~26%).[21] This difference can be understood if we take into account that not all NC facets can be terminated

Received: April 17, 2014
Published: July 28, 2014

   dx.doi.org/10.1021/ja503866w | *J. Am. Chem. Soc.* 2014, 136, 11228−11231

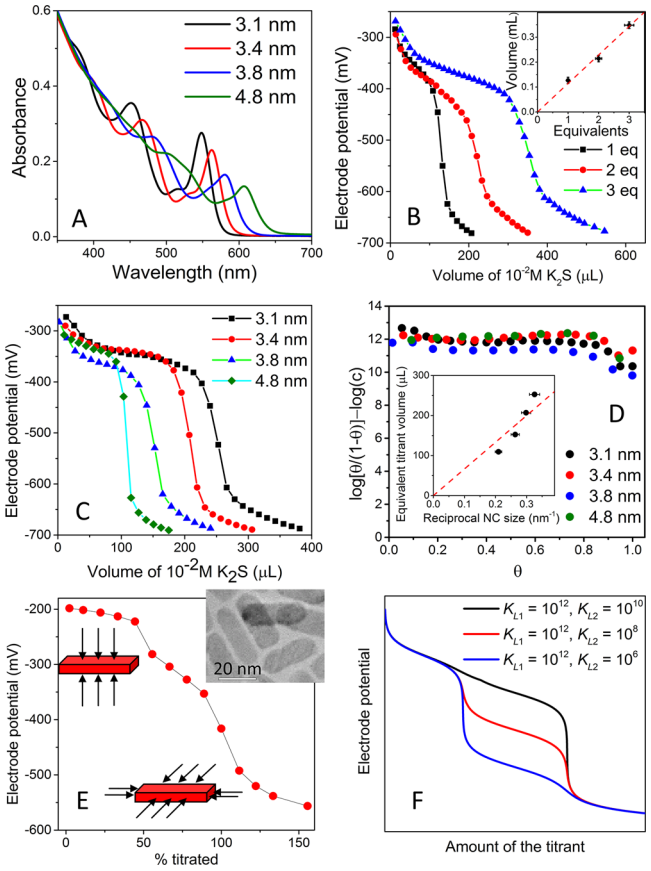

Figure 1. (A) Absorption spectra of CdSe QDs of different sizes. (B) Titration curves of three aliquots—1.22, 2.44, and 3.66 mg—of $[CdSe/Cd^{2+}]^{n+}nBF_4^-$ NCs with K_2S in NBu_4ClO_4/NMF. Inset: The equivalent amount of the titrant is proportional to the amount of the QDs taken for the titration. (C) Titration curves for the aliquots of CdSe QDs of different sizes, all normalized per mass of CdSe. (D) Quantitative analysis of the titration curves from panel (C) using FFG isotherm. The inset shows that the equivalent amount of the titrant decreases with increasing NC size. (E) Titration curve for CdSe@CdS nanoplatelets with two monolayers of CdS on each side. (F) Calculated titration curves for Langmuir adsorption with two equivalence points.

exclusively by Cd surface sites and that sulfide ion can coordinate to more than one Cd site on the surface. In the process of titration there is a recharging of the NC surface, which has been studied[14] and implemented in the colloidal atomic layer deposition (*c*-ALD) technique.[22]

Next, we titrated aliquots of $[CdSe/Cd^{2+}]^{n+}nBF_4^-$ NCs of four different sizes. The absorbance of each solution was adjusted to the same value at 350 nm (Figure 1A); therefore, the total mass of CdSe in each titrated solution was the same. Figure 1C shows that the equivalent amount of the titrant is larger for smaller QDs. This makes perfect sense since the total surface area in the colloidal solution of smaller QDs is greater than that in the solution of larger QDs. The equivalent amount of the titrant is not perfectly proportional to the expected reciprocal particle size, deviating upward at smaller particle sizes (Figure 1D, inset). We think this discrepancy lies in the oversimplified view of a QD as a simple spherical object. Non-stoichiometric surface terminations, roughness, and surface reconstructions can increase the number of adsorption sites for smaller particles. In fact, recent stoichiometry studies of CdSe NCs revealed a stronger deviation from 1:1 composition in smaller NCs.[23] Similar behavior was observed for $[CdSe/Cd^{2+}]^{n+}nBF_4$ NCs used in this study (Table S1).

Equilibrium constants for the ligand binding to the NC surface can be estimated by making an analogy with adsorption isotherms that describe equilibria between free and surface-bound species. The simplest Langmuir adsorption model defines the binding constant as $K_L = \theta/[(1-\theta)c]$, where θ is the surface coverage and c is the equilibrium concentration of the free species. The Frumkin–Fowler–Guggenheim (FFG) isotherm accounts for possible repulsion between charged adsorbed ligands: $\theta/(1-\theta)c = K_L \exp(-sU_p\theta/k_BT)$, where U_p is the ligand–ligand interaction energy, s is the ligand coordination number in a fully covered surface, k_B is the Boltzmann constant, and T is the absolute temperature.[24] When $\upsilon = 0$, FFG reduces to the Langmuir isotherm.

In Figure 1D, the FFG isotherm is linearized in $\log\{\theta/[(1-\theta)c]\}$ vs θ coordinates for the four titration curves shown in Figure 1C. The slope of the obtained line is the interaction parameter $\upsilon = -sU_p\theta/(k_BT)$, and the intercept is $\log K_L$. First, we noticed that all CdSe QDs show similar $K_L \approx 10^{12}$, with no apparent size dependence. In a broad range of θ values, $\upsilon \approx 0$ suggests that accumulation of negative charge at the NC surface due to the adsorption of S^{2-} ions does not affect binding up to $\theta \approx 0.8$. This observation makes sense because we are dealing with crystal layer growth and not physical adsorption. $K_L \approx 10^{12}$ indicates a high affinity of S^{2-} for the CdSe surface and thus high surface coverage and lower equilibrium concentration of free ligands at the equivalence point. In particular, for the 4.8 nm CdSe QDs, the electrode potential at the equivalence point was −523 mV, which corresponds to the equilibrium concentration of free S^{2-} of 1×10^{-7} M and very close to unity surface coverage.[17] Colloidal NCs are terminated with different facets that may exhibit differences in reactivity, which is used in synthesis of anisotropic nanostructures like nanorods[25] or nanoplatelets (NPLs).[26] The ability to measure and exploit the difference in facet reactivity would open up new prospects for synthesis of complex nanomaterials. As an example of highly anisotropic nanostructure, we used CdSe@CdS core–shell NPLs (Figure 1E). The span of the electrode potential was similar to that for spherical CdSe QDs. The titration curve for the NPLs showed two distinct steps, which could result from the different K_L values for different facets. We hypothesize that the large (001) facets of CdSe NPLs[27] have higher affinity for S^{2-} ions. Indeed, for the highly anisotropic growth to occur during the NPL synthesis, these facets must be heavily passivated with carboxylate ligands, hence, Cd-rich. After removal of the carboxylate ligands with Me_3OBF_4, these facets expose the highest concentration of electrophilic metal sites and exhibit high reactivity. As a word of caution, our modeling shows that, to clearly resolve multiple equivalence points, the difference between K_L values should reach orders of magnitude, with the smallest K_L at least of the order of 10^6 (Figure 1F).[17]

In situ potentiometry can be applicable to various colloidal nanomaterials. For example, Figure 2A compares titration curves for CdSe and InP QDs of similar sizes.[17] The potential drop around the equivalence point was shallower for InP QDs. Figure 2B shows modeled titration curves corresponding to different K_L values. Analysis identical to that shown in Figure 1E results in the estimated $K_L \approx 10^{10}$ for InP, 2 orders of magnitude lower than that for CdSe. This difference suggests that In^{III} sites at the InP QD surface show lower affinity for sulfide ions compared to Cd^{II} sites at CdSe QD surface.

dx.doi.org/10.1021/ja503866w | J. Am. Chem. Soc. 2014, 136, 11228–11231

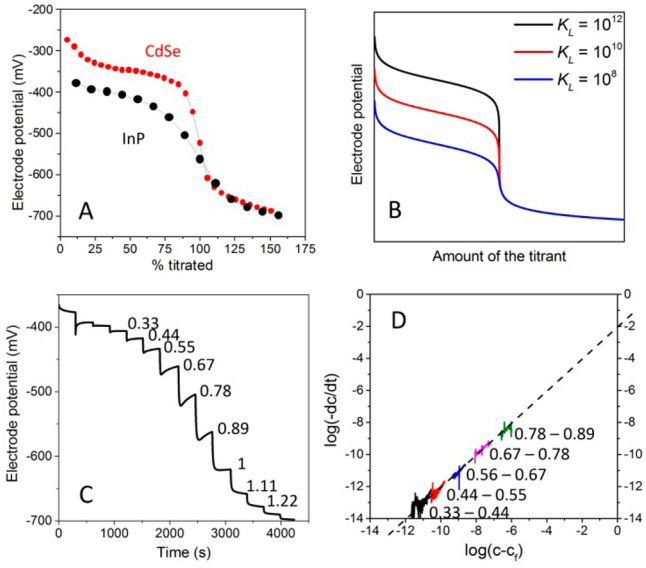

Figure 2. (A) Potentiometric titration curves for CdSe and InP QDs of similar size. (B) Calculated titration curves for Langmuir adsorption with different K_L values. (C) The electrode potential as a function of time in a titration of InP QDs with K_2S. (D) Log–log plot of the differential rate law to estimate the reaction order and the rate constant for reaction of S^{2-} with the surface of InP QDs. The numbers correspond to surface coverage, θ.

Surface Reaction Kinetics. *In situ* potentiometry can also provide an insight into the reaction kinetics at NC surface. In the previous analysis, we used equilibrium values of the electrode potential, typically recorded 5 min after addition of S^{2-} solution. However, the dynamics of electrode response following the injection of S^{2-} (Figure 2C) can provide additional information. To illustrate this we used reaction of InP QDs with S^{2-}. The kinetics of ligand adsorption at the surface of InP QDs depends largely on the region of the titration curve. Until about halfway to the equivalence point, injection of the titrant resulted in downward spikes of the electrode potential, followed by fast recovery to the equilibrium value. When the amount of injected sulfide was between 50 and 100%, the initial potential drop became deeper and the recovery was slower. Past the equivalence point, no spikes were observed, and potential was determined by the electrode response to ever increasing concentrations of S^{2-} (Figure 2C).

Ligand adsorption in the $0.33 < \theta < 1$ region was analyzed quantitatively. In the simplest case, for reversible ligand adsorption, the rate of change of the concentration of free S^{2-} ions, c, is given by the differential rate law $-dc/dt = k_{eff}(c - c_f)^n$, where the effective rate constant, k_{eff}, depends on θ and the NC concentration, c_f is the concentration of free S^{2-} ions when equilibrium establishes, and n is the reaction order in S^{2-}. We analyze the adsorption kinetics for the five ligand injections before the equivalence point. All five separate data sets obey first-order kinetics in S^{2-} (Figure 2D), all with $k_{eff} \approx 10^{-2}$ s^{-1}. For this specific example, it takes 230 s for 90% of the injected ligands to react with the InP QD surface at 300 K. CdSe QDs showed significantly faster reaction with S^{2-} ions, so extraction of reliable k_{eff} values would require faster electrode response than that used in our study.

Probing NC Surface in Nonpolar Solvents. In the above examples, the chemical manipulations with NCs were performed and monitored in a polar medium. In contrast, most syntheses and transformations of colloidal NCs are carried out in nonpolar solvents such as 1-octadecene (ODE), often at elevated temperature. The use of potentiometry under such conditions could provide important information such as the total active surface area for NCs of different size, shape, and composition. Knowledge of the surface area is needed in quantitative description of chemical processes at a NC surface during synthesis, ligand binding, or conjugation reactions. If we had a feedback mechanism to follow surface reactions, we could stop addition of reactants exactly at the equivalence point or even after reacting certain facets while keeping other facets intact. In particular, it would have an important implication to SILAR[28,29] and *c*-ALD[22] techniques for synthesis of nano-heterostructures.

Direct potentiometry in nonpolar media would be challenging.[19] We therefore designed an experiment in which we monitored the surface of NCs dispersed in a nonpolar phase (hexane) while tracking the concentration of free ligands in the polar phase (formamide, FA) in direct contact with the NC solution (Figure 3A). To facilitate transfer of S^{2-} ions across

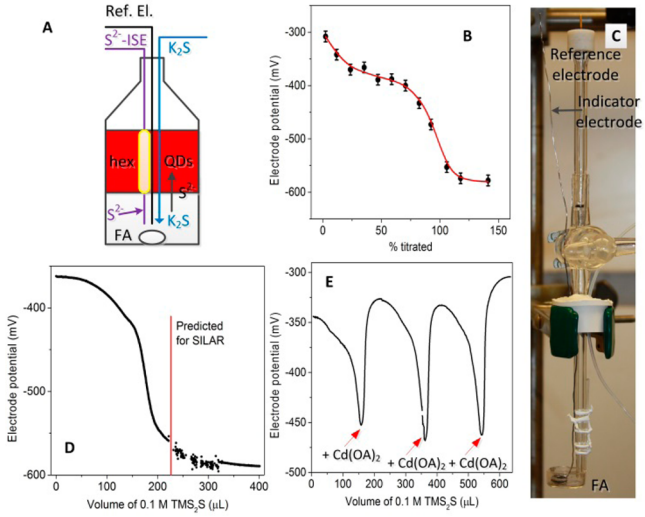

Figure 3. (A) Approach used to potentiometrically probe colloidal NCs in nonpolar solvents. (B) Titration of w-CdSe QDs dispersed in the upper (hexane) phase with K_2S/FA injected into the FA phase. (C) Photograph of the accessory that inserts into a standard three-neck flask equipped with a reflux condenser and temperature sensor.[17] (D) Titration of w-CdSe QDs in ODE with TMS_2S in oleylamine at 150 °C. (E) SILAR synthesis of CdSe@CdS core–shell QDs using real-time monitoring of reaction by potentiometry.

the phase boundary between FA and hexane, we added oleylamine (OAm), which formed oleylammonium sulfide that was soluble in the hexane phase. $(NH_4)_2S$ can either be injected to the FA phase or first reacted with OAm and then injected directly into the hexane phase with dispersed colloidal NCs (Figure S6).[17] When the equilibrium distribution of S^{2-} between two phases established, the concentration of free S^{2-} in the nonpolar phase was proportional to that in the polar phase through the distribution constant: $[S^{2-}]_{hex} = K_{distr}[S^{2-}]_{FA}$. The logarithm of the distribution constant appeared as an offset in the electrode potential; therefore, although the titration curve was shifted vertically, its shape was not altered. Slow kinetics of the ligand transfer across the phase boundary appears to be the main limiting factor for this approach. To overcome this limitaton and study the NC surface under

dx.doi.org/10.1021/ja503866w | J. Am. Chem. Soc. 2014, 136, 11228–11231

realistic conditions, we designed a small glass cup attached to a capillary filled with 10^{-2} M $LiClO_4$/FA so that the tip of the capillary was immersed in a thin layer of FA solution on the bottom of the cup (Figure 3C). The indicator electrode was immersed in $LiClO_4$/FA on the bottom of the cup, while the reference electrode was immersed in the solution of electrolyte at the top of the capillary.[17] We thus established a circuit, Ag/Ag_2S electrode|$LiClO_4$/FA on the bottom of the cup|$LiClO_4$/FA, in the capillary|reference electrode. The thin layer of the electrolyte solution was in contact with the ODE solution of QDs, and thus, via the distribution constant, we probed the concentration of S^{2-} in the ODE phase at 150 °C, which is close to experimental conditions for the synthesis of CdSe/CdS core−shell NCs. In a typical run we titrated an aliquot of w-CdSe QDs (Figure 3D) or zb-CdSe NPLs (Figure S10) with $[(CH_3)_3Si]_2S$ in ODE. In Figure 3C, the equivalence point was clearly observable 10 min from the beginning of the titration. The experiment required 175 μL of the titrant to reach the equivalence point. In a typical SILAR synthesis, deposition of the first sulfide layer would require 228 μL of the titrant,[17,28,30] so the experimental results agreed fairly well with the prediction. The fact that not all facets of w-CdSe NCs are (0001), as it is implied in the calculation, makes the required amount of the titrant lower than 228 μL. This information can be used to correct the amounts of precursors for SILAR and c-ALD techniques and prevent secondary nucleation, a typical problem in synthesis of core−shell nanostructures.[29]

Finally, we demonstrate practical utility of potentiometry for core−shell growth via controlled layer-by-layer deposition of CdS shells. In the previous experiment, we noticed that the electrode potential at the equivalence point was between −450 and −500 mV, so, in a typical titration experiment, we injected the equivalent amount of Cd oleate when the potential reached −450 mV. After the injection, the electrode potential grew sharply and then continued to follow a regular titration curve (Figure 3D). We controllably grew three layers of CdS. The resulting solution showed expected red shifts in the absorption and emission spectra and high photoluminescence efficiency. TEM images also showed no evidence of secondary nucleation of CdS (Figure S11).

To summarize, potentiometry is a powerful technique for *in situ* studies of a nanomaterial's surface. Here we used a S^{2-}-selective electrode, but our approach can be easily extended to other ions by using suitable ion-selective electrodes. We believe that other DC and AC electrochemical techniques such as voltammetry, amperometry, and conductometry can be used to monitor various chemical processes during NC synthesis and post-synthetic treatments.

■ ASSOCIATED CONTENT

Supporting Information

Experimental details and supporting figures. This material is available free of charge via the Internet at http://pubs.acs.org.

■ AUTHOR INFORMATION

Corresponding Author

dvtalapin@uchicago.edu

Notes

The authors declare no competing financial interest.

■ ACKNOWLEDGMENTS

We thank Sandrine Ithurria for advice on NC synthesis, J. Matthew Kurley for help with the experimental setup, and Dmitriy S. Dolzhnikov for advice on the electrode preparation. This work was supported by NSF under Award No. DMR-1310398 and by DOD ONR under Award No. N00014-13-1-0490. D.V.T. also thanks the David and Lucie Packard Foundation and Keck Foundation for support. This work used facilities supported by NSF MRSEC Program Award No. DMR 08-20054. Use of the Center for Nanoscale Materials was supported by the U.S. Department of Energy, Office of Science, Office of Basic Energy Sciences, under Contract No. DE-AC02-06CH11357.

■ REFERENCES

(1) Colvin, V. L.; Schlamp, M. C.; Alivisatos, A. P. *Nature* **1994**, *370*, 354.
(2) Chung, D. S.; Lee, J.-S.; Huang, J.; Nag, A.; Ithurria, S.; Talapin, D. V. *Nano Lett.* **2012**, *12*, 1813.
(3) Gur, I.; Fromer, N. A.; Geier, M. L.; Alivisatos, A. P. *Science* **2005**, *310*, 462.
(4) Bharali, D. J.; Lucey, D. W.; Jayakumar, H.; Pudavar, H. E.; Prasad, P. N. *J. Am. Chem. Soc.* **2005**, *127*, 11364.
(5) Chen, M. S.; Goodman, D. W. *Science* **2004**, *306*, 252.
(6) Talapin, D. V.; Lee, J.-S.; Kovalenko, M. V.; Shevchenko, E. V. *Chem. Rev.* **2009**, *110*, 389.
(7) Ling, W. L.; Hamilton, J. C.; Thürmer, K.; Thayer, G. E.; de la Figuera, J.; Hwang, R. Q.; Carter, C. B.; Bartelt, N. C.; McCarty, K. F. *Surf. Sci.* **2006**, *600*, 1735.
(8) Neave, J. H.; Joyce, B. A.; Dobson, P. J.; Norton, N. *Appl. Phys. A: Mater. Sci. Process.* **1983**, *31*, 1.
(9) Tuinenga, C.; Jasinski, J.; Iwamoto, T.; Chikan, V. *ACS Nano* **2008**, *2*, 1411.
(10) Dagtepe, P.; Chikan, V.; Jasinski, J.; Leppert, V. J. *J. Phys. Chem. C* **2007**, *111*, 14977.
(11) Coronado, J. M.; Kataoka, S.; Tejedor-Tejedor, I.; Anderson, M. A. *J. Catal.* **2003**, *219*, 219.
(12) Hens, Z.; Martins, J. C. *Chem. Mater.* **2013**, *25*, 1211.
(13) Polte, J.; Ahner, T. T.; Delissen, F.; Sokolov, S.; Emmerling, F.; Thünemann, A. F.; Kraehnert, R. *J. Am. Chem. Soc.* **2010**, *132*, 1296.
(14) Nag, A.; Kovalenko, M. V.; Lee, J. S.; Liu, W. Y.; Spokoyny, B.; Talapin, D. V. *J. Am. Chem. Soc.* **2011**, *133*, 10612.
(15) Rosen, E. L.; Buonsanti, R.; Llordes, A.; Sawvel, A. M.; Milliron, D. J.; Helms, B. A. *Angew. Chem., Int. Ed.* **2012**, *51*, 684.
(16) Qu, L. H.; Peng, Z. A.; Peng, X. G. *Nano Lett.* **2001**, *1*, 333.
(17) Details are provided in the Supporting Information.
(18) Dobcnik, D.; Gros, I.; Kolar, M. *Acta Chim. Slov.* **1998**, *45*, 209.
(19) Izutsu, K. *Electrochemistry in Nonaqueous Solutions*; Wiley-VCH Verlag GmbH & Co. KGaA: Weinheim, 2009.
(20) Gomes, R.; Hassinen, A.; Szczygiel, A.; Zhao, Q.; Vantomme, A.; Martins, J. C.; Hens, Z. *J. Phys. Chem. Lett.* **2011**, *2*, 145.
(21) Smith, A. M.; Nie, S. *Acc. Chem. Res.* **2009**, *43*, 190.
(22) Ithurria, S.; Talapin, D. V. *J. Am. Chem. Soc.* **2012**, *134*, 18585.
(23) Luther, J. M.; Pietryga, J. M. *ACS Nano* **2013**, *7*, 1845.
(24) Butt, H.-J., Graf, K., Kappl, M. *Physics and Chemistry of Interfaces*; Wiley-VCH Verlag GmbH & Co. KGaA: Weinheim, 2006.
(25) Manna, L.; Scher, E. C.; Alivisatos, A. P. *J. Am. Chem. Soc.* **2000**, *122*, 12700.
(26) Ithurria, S.; Dubertret, B. *J. Am. Chem. Soc.* **2008**, *130*, 16504.
(27) Ithurria, S.; Bousquet, G.; Dubertret, B. *J. Am. Chem. Soc.* **2011**, *133*, 3070.
(28) Li, J. J.; Wang, Y. A.; Guo, W. Z.; Keay, J. C.; Mishima, T. D.; Johnson, M. B.; Peng, X. G. *J. Am. Chem. Soc.* **2003**, *125*, 12567.
(29) Tan, R.; Blom, D. A.; Ma, S.; Greytak, A. B. *Chem. Mater.* **2013**, *25*, 3724.
(30) de Mello Donegá, C.; Koole, R. *J. Phys. Chem. C* **2009**, *113*, 6511.